Nanotechnology **20** (2009) 395501 (5pp) doi:10.1088/0957-4484/20/39/395501

High-performance humidity sensors based on high-field anodized porous alumina films

Lujun Yao[1], Maojun Zheng[1,4], Haibin Li[2], Li Ma[3] and Wenzhong Shen[1]

[1] Laboratory of Condensed Matter Spectroscopy and Opto-Electronic Physics, Department of Physics, Shanghai Jiao Tong University, Shanghai 200240, People's Republic of China
[2] Institute of Fuel cell, School of Mechanical Engineering, Shanghai Jiao Tong University, Shanghai 200240, People's Republic of China
[3] School of Chemistry and Chemical Technology, Shanghai Jiao Tong University, Shanghai 200240, People's Republic of China

E-mail: mjzheng@sjtu.edu.cn

Received 28 April 2009, in final form 27 July 2009
Published 2 September 2009
Online at stacks.iop.org/Nano/20/395501

Abstract
Improved humidity sensors based on porous anodized alumina (PAA) films were prepared via stable high-field anodization and subsequent isotropic chemical etching for appropriate times. The results reveal that sensitivity over a wide humidity range can be adjusted by changing the microstructure of the porous alumina layer, which can be explained in terms of the inhomogeneous distribution of anion impurities in the pore sidewall. The short response and recovery times obtained were ascribed to the ordered pore arrays and large pore size of the PAA films. This study has significance in tailoring the moisture sensitivity in the design of diverse sensors for practical applications.

(Some figures in this article are in colour only in the electronic version)

1. Introduction

Electrochemically produced porous anodic alumina (PAA) films [1, 2] have been extensively used as host or template structures for the fabrication of diverse nanometer devices, such as electronic [3], magnetic [4] and photonic [5] devices. Their application as a promising material in humidity sensors has also attracted much attention since the influence of water vapor on electrical properties was first reported by Ansbacher and Jason [6] in 1953. In recent years, humidity sensors based on nano-structured alumina thin films [7–10] and other nanometer materials [11] prepared by different methods have also been reported. Compared with other humidity sensors, the advantages of an Al_2O_3 humidity sensor arise from simple, low-cost fabrication, thermal and physical stability [12]. Several studies have been made to investigate the performance of the thin film porous alumina moisture sensor and to understand the surface conduction mechanism [13, 14] which controls the sensitivity characteristics. However, the humidity sensor reported by other authors [13–16] mainly shows the characteristic in which the capacitance increases slowly with relative humidity (RH) rising up to 40%–50% and then just shows a sharp increase. This type of sensor suffers from insufficient sensitivity over a wide humidity range and could not satisfy the demands of their applications at low humidity. We note that in preparing sensors with PAA thin films, they have all in the past been fabricated in normal field, i.e. low current anodizing. In this paper, we present a method to obtain improved humidity sensors based on the self-organized porous alumina thin films by stable high-field anodization in a H_3PO_4–H_2O–C_2H_5OH system [17–21]. It was interesting that sensors with PAA film pretreatment via isotropic chemical etching showed improved sensitive performance at low humidity and the sensitivity over a wide humidity range could be modulated, which is helpful in tailoring the moisture sensitivity to design sensors for a diverse gamut of automated industrial manufacturing and agricultural equipment and other instrumentation according to the actual

[4] Author to whom any correspondence should be addressed.

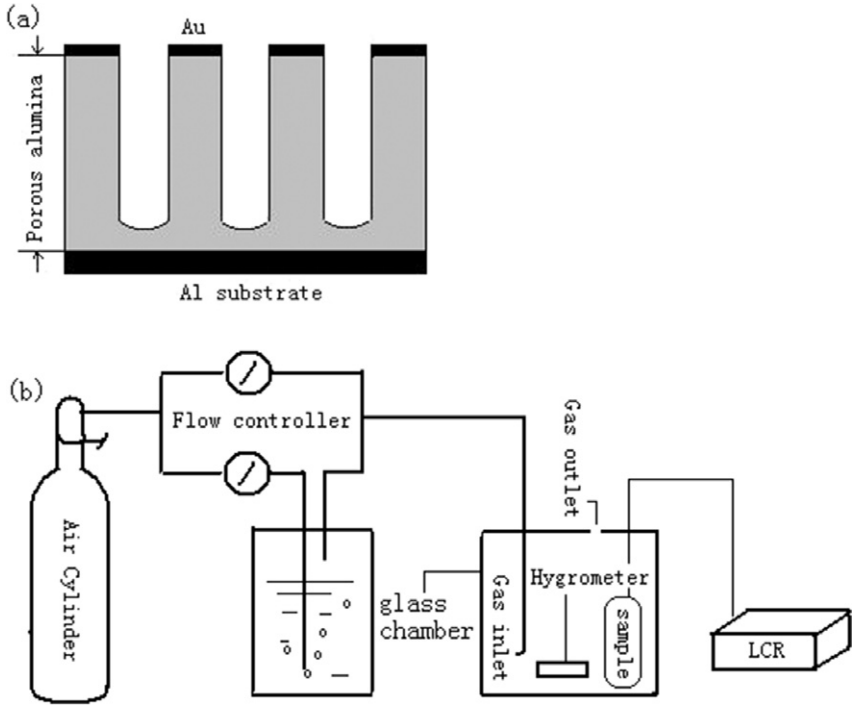

Figure 1. (a) The structure sketch of the Al_2O_3 humidity sensor and (b) the schematic of the experimental setup where the RH can be obtained in the glass chamber.

application [12]. In addition, short response and recovery times were also obtained as excellent parameters for a sensor device.

2. Experimental details

The experiments mainly consist of two parts: the formation of PAA films, sensor fabrication and the measurements of sensor capacitance as a function of RH.

2.1. The formation of PAA films

A slice of aluminum (99.999% purity, 0.25 mm thickness) was cut into some circular foils with a radius of 1 cm, degreased in acetone, washed in deionized water and dried off with nitrogen gas. Then the circular foils were put into a tailor-made holder with a circular area of 2 cm^2 exposed to the electrolyte. The power supply (Agilent, N5752A) was used to keep the voltage constant. Before anodization, the aluminum was electropolished at a constant voltage in a solution mixture of perchloric acid and ethanol ($HClO_4$:C_2H_5OH = 1:4 v/v) for several minutes to improve the smoothness of the surface. The temperatures of the electrolytes were kept at −10–0 °C. The electrolytes (C_2H_5OH:H_2O = 1:4 v/v) can be sulfuric acid (0.2 M), oxalic acid (0.3 M) in the normal-field case and phosphoric acid (0.4 M) in the high-field case. The first anodization step lasted for 2 h for the normal case or several minutes for the high-field case to form regular hexagonal pore arrays. Then to dissolve the orderless surface, the foils were immersed in a mixture of 6 wt% phosphoric acid and 1.8 wt% chromic acid at a temperature of 60 °C for the proper time. Then followed the second anodization with the same conditions as the first step, the anodization times are 2 h for sulfuric acid, 5 h for oxalic acid and 2 min for phosphoric acid. In contrast to the former ones, the nanopore arrays are highly uniform. The as-grown PAA films fabricated in phosphoric acid under a high field of 195 V have an initial pore diameter of 180 nm. Subsequently, their pore diameters were increased by isotropic chemical etching in 5 wt% phosphoric acid at 45 °C for different times to get a diverse value of the last pore diameters. The morphology of the samples was observed using a field-emission scanning electron microscope (FE-SEM, Philips Sirion 200).

2.2. Sensor fabrication and measurements

On one side of the anodized surface a circular gold film about 40 nm thick and 8 mm in diameter was deposited as one of the two electrodes by ion sputtering. The other electrode was unanodized aluminum foil. Copper wires were connected to the two electrodes using conducting silver glue. The structure sketch of the porous alumina humidity sensor is shown in figure 1(a). The schematic of the experimental setup is exhibited in figure 1(b), RH conditions of 5%–95% were obtained in a glass chamber and with the hygrometer (Beijing, WS508D) as the reference sensor. The RHs were generated by bubbling dry air from an air cylinder through pure water and adjusting the flow rates of dry air and wet air. Sensor capacitance was measured until the RH was in a steady condition for about 15 min. The temperature of the experimental environment was maintained at 20 °C. Measurements of sensor capacitance were performed with the frequency at 1 kHz and an amplitude of 1 V using an LCR meter (Agilent, 4284A).

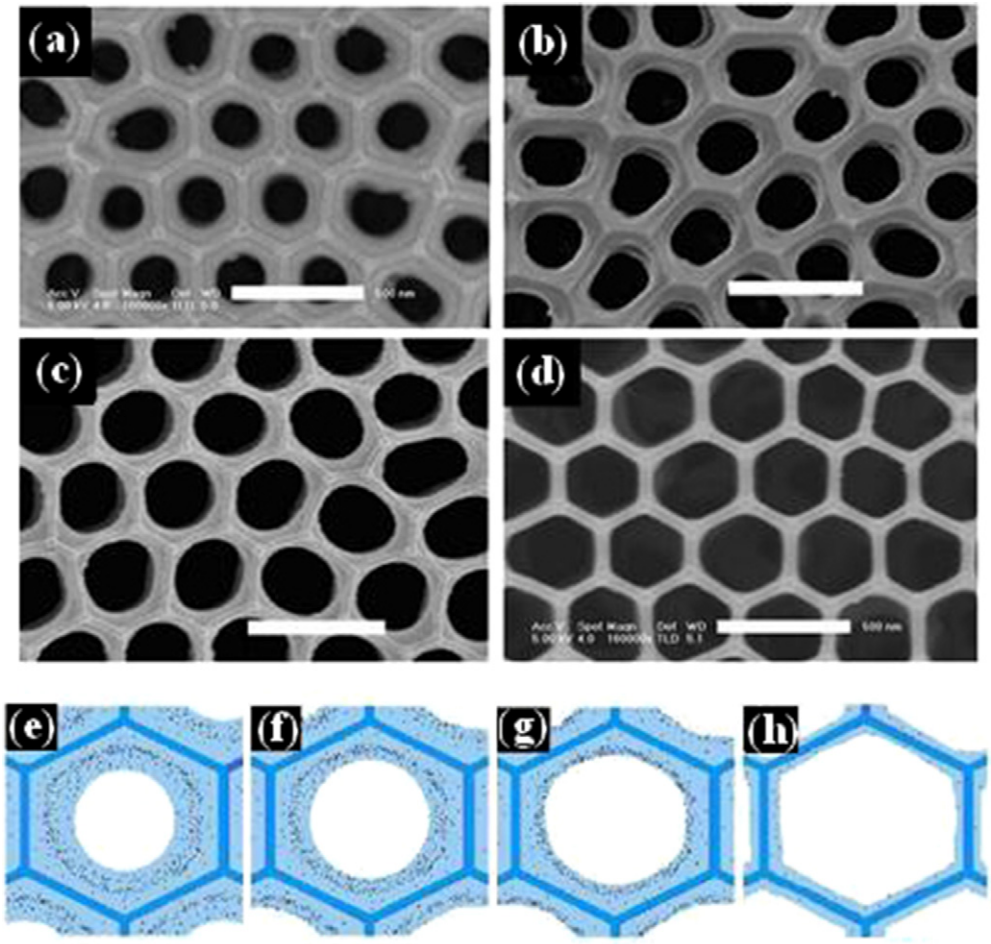

Figure 2. FE-SEM images (top view) of the samples with different chemical etching time: (a) 0 min, (b) 15 min, (c) 30 min and (d) 40 min; (e)–(h) are the corresponding sketches of the distribution of anion impurities. The length of the inserted scale bars is 500 nm.

3. Results and discussion

Figures 2(a)–(d) exhibit the typical FE-SEM images of the PAA thin films fabricated in phosphoric acid solution under a high field of 195 V and their subsequent chemical etching for appropriate times. The as-grown PAA films have a uniform pore structure and thick pore sidewall, as shown in figure 2(a). Since the pore sidewall is thick enough compared with the PAA film made in normal field, the pore size is more easily controlled on the large scale without destroying the pore structure but also it is feasible to change the anion impurity concentration in the pore sidewall surface by isotropic chemical etching for the proper length of time, which is convenient for us to study the influence of anion concentration on sensor characteristics because the surface conduction mechanism is related to anion impurities incorporated into the pore sidewall. Many studies have revealed that the distribution of anion concentration in the PAA pore sidewall is inhomogeneous [22–24] and the porous alumina has two duplex structure: an inner oxide layer composed of pure alumina and an outer oxide layer with anion impurities [25] such as O^{2-}, OH^{-} and PO_4^{2-}. Furthermore, the outer oxide layer also consists of an outermost oxide part and an intermediate oxide part and most of the anion impurities are distributed in the intermediate part of the outer layer. Here, we choose the four samples with chemical etching time 0, 15, 30 and 40 min on the basis of the anion concentration distribution and the expansion rate of pore sizes [26]. The sketch of the anion impurities distribution of PAA cells is shown in figures 2(e)–(h).

Figure 3 represents the experimental characteristics of capacitance as a function of RH for the above four samples. They exhibit a well-behaved change in capacitance about a magnitude of 10^2–10^3 over the 5% to 95% RH range. The sensitivity of as-prepared sensors with chemical etching shifts the operating range to lower humidity values. The as-prepared sensors also enjoy an apparent advantage over the normal-field sensors prepared in this work as the latter suffered from insensitivity at low humidity, as presented in the inset. For the sensors with chemical etching time 0 min, 15 min, 30 min and 40 min, their sensitivities (defined as: $S = C_{(\mathrm{RH}=85\%)}/C_{(\mathrm{RH}=35\%)}$) are enhanced from 29, 75, 192 to 348 one by one and the capacitance begins to increase remarkably when the RH rises up to 55%, 35%, 20% and 35% respectively, while the values are 40% and 60% for the studied sulfuric acid and oxalic acid sensor.

The above phenomenon should mainly arise from the inhomogeneous distribution of anion concentration, and other

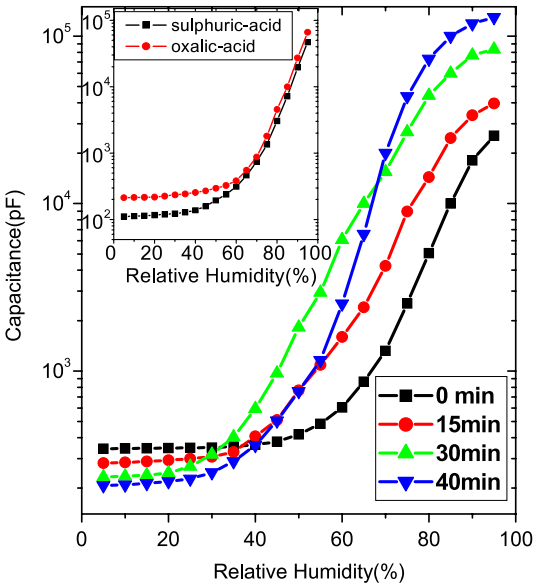

Figure 3. Capacitance characteristics of phosphoric acid sensors based on the high-field PAA thin films. The inset shows the capacitance characteristics of a sulfuric acid and oxalic acid sensor prepared in normal field.

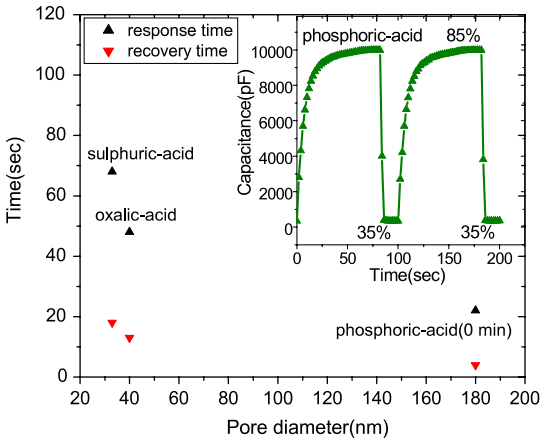

Figure 4. The response time (▲) and recovery time (▼) of three sensors with different pore diameters 33 nm, 40 nm and 180 nm. The inset is the typical response/recovery graph of the phosphoric acid sensor without chemical etching.

parameters such as pore size [27] are also of importance in controlling the sensitivity characteristics. When the RH is zero, the conduction on the porous alumina layer is electronic. As the humidity increases, water molecules are adsorbed to the anion sites incorporated in the pore sidewall surface and form a monolayer gradually, which leads to the reduction of the surface potential barrier and a decrease in the interface state density. Generally, the dominant conduction mechanism in the low humidity range is electronic conduction. The surface conductivity in this range can be represented [13, 28]

$$\sigma_{\mathrm{w}} = \sigma_0 \exp(-2r/\delta - E_a/K_{\mathrm{B}}T) \qquad (1)$$

where σ_0 is a constant, r is the distance between the anionic sites and is equal to the tunneling distance and δ is the localization length of the water state. In a pore sidewall surface having more anions, the anions will be closely spaced, so σ_{w} will be much higher. The inset of figure 3 shows that the capacitance versus RH has a flat response at low humidity for an oxalic acid sensor. It has been shown that during anodizing substantial quantities of anion enter the film in sulfuric acid and only moderate amounts in oxalic acid [29]. Based on the aforesaid theory, in the PAA film without chemical etching (figure 2(e)), the anion impurities in the pore sidewall surface are few so that the surface conduction σ_{w} is hardly improved and the variation of capacitance is tiny. When the pore diameter was increased by isotropic chemical etching for 15 and 30 min (figures 2(f) and (g)), the anion concentration in the pore sidewall surface increased gradually, which improved the surface conductivity and thereby led to the sensitive characteristics at low humidity. However, when the PAA thin film was etched for 40 min (figure 2(h)), the outer oxide layer was nearly dissolved, while the concentration of anion impurities became small again and the pore surface conduction σ_{w} decreased and then caused the degradation of sensitivity compared with that etched for 30 min.

At high humidity, many water molecules are adsorbed and diffuse into the pore sidewalls to form a thin water layer on the alumina surface and the proton transmission in this thin water layer dominates the conduction process. When the RH is high enough, the whole porous alumina layer is nearly wetted by the adsorbed water resulting in a loss of pore dielectric isolation among the pores, especially for the sample with thinner pore sidewalls. Hereafter the sensor capacitance in such cases will be decided mainly by the barrier layer, which can be estimated by the formula for capacitance ($C = \varepsilon_{\mathrm{r}}\varepsilon_0 S/d_{\mathrm{bar}}$ where ε_{r}, d_{bar} represent the relative dielectric constant and thickness of alumina barrier layer, respectively). The theoretical values estimated by the formula for capacitance are also approximately equal to those of experimental results. Moreover, from figure 3 we also know that with the increasing etching time (pore diameter is larger) the curve shows a flat response more clearly at high RH. This phenomenon was not found for the previously studied sensor. So we conclude that the pore size of PAA films fabricated in phosphoric acid solution under high field and chemical etching is larger, making it easier for the water molecules to get to the barrier layer and fill the whole porous alumina layer. Based on this analysis, chemical etching can be considered as a useful method to improve the sensitivity.

Further studies of response and recovery time were carried out for dynamic testing procedures, which provided more information on the most important parameters for a sensing device. The response time, defined as the time needed to reach 90% of the final signal for a given RH, and recovery time, defined as the time taken for the signal to come within 10% of the initial value, were determined by alternately exposing these sensors to a 35% or 85% RH ambient with capacitance measured at a frequency of 1 kHz. Figure 4 represents the experimental value of an as-prepared phosphoric acid sensor (0 min) for the high-field case, and sulfuric acid and oxalic acid sensors for the normal-field case. We observe that the

phosphoric acid sensor has the shortest response and recovery time, the inset shows its response/recovery graph and we can see that $\tau_{res} \approx 24$ s and τ_{rec} is less than 4 s. The recovery time τ_{rec} is much shorter than τ_{res} which has rarely been reported before. The first explanation for this remarkable change might be that the as-grown sensor with the PAA film fabricated in high field has large pore size and high-quality self-ordered pore structure, which avoids the appearance of capillary condensed water according to the Kelvin equation and water molecules can be adsorbed or desorbed easily to get a balance.

4. Conclusion

We have prepared humidity sensors using porous anodized alumina films fabricated by stable high-field electrochemical oxidation of aluminum. This sensor shows short response and recovery times due to large pore size. Based on the high-field PAA films, the humidity-sensitive region of operation and the sensitivity over a wide humidity range can be adjusted by isotropic chemical etching for the appropriate time. That a definite correlation exists between the moisture sensitivity characteristics at low humidity and the concentration of anion impurities in the pore sidewall surface was studied. The optimal preparation procedure in our work was for sensors fabricated with PAA films via stable high-field anodization in the H_3PO_4–H_2O–C_2H_5OH system at 195 V and subsequent isotropic chemical etching for about 30 min. This work provides an approach to improve the performance of humidity sensors.

Acknowledgments

This work was supported by the Natural Science Foundation of China (grant Nos 10874115, 50672058), Shanghai Key Basic Research Project of 08JC1411000 and Shanghai Nanotechnology Research Project 0952nm01900. We thank the Instrumental Analysis Center of SJTU for SEM analysis.

References

[1] Masuda H and Fukuda K 1995 *Science* **268** 1466
[2] Lee W, Schwirn K, Steinhart M, Pippel E, Scholz R and Gösele U 2008 *Nat. Nanotechnol.* **3** 234
[3] Liu C H, Yiu W C, Au F C K, Ding J X, Lee C S and Lee S T 2003 *Appl. Phys. Lett.* **83** 3168
[4] Nielsch K, Müller F, Li A P and Gösele U 2000 *Adv. Mater.* **12** 582
[5] Nishio K and Masuda H 2004 *Electrochem. Solid-State Lett.* **7** H27
[6] Ansbacher F and Jason A C 1953 *Nature* **171** 177
[7] Steele J J, Gospodyn J P, Sit J C and Brett M J 2006 *IEEE Sensors J.* **6** 24
[8] Madany A, Jasiński P, Jasiński G, Chachulski B and Nowakowski A 2006 *Proc. SPIE* **6348** 63480C
[9] Saha D, Mistry K K, Giri R, Guha A and Sensgupta K 2005 *Sensors Actuators* B **109** 363
[10] Dickey E C, Varghese O K, Ong K G, Gong D, Paulose M and Grimes C A 2002 *Sensors* **2** 91
[11] Wang J, Wang X H and Wang X D 2005 *Sensors Actuators* B **108** 445
[12] Traversa E 1995 *Sensors Actuators* B **23** 135
[13] Nahar R K, Khanna V K and Khokle W S 1984 *J. Phys. D: Appl. Phys.* **17** 2087
[14] Khanna V K and Nahar R K 1987 *Appl. Surf. Sci.* **28** 247
[15] Kovac M G, Chleck D and Goodman P 1978 *Solid State Technol.* **21** 35
[16] Nahar R K 2000 *Sensors Actuators* B **63** 49
[17] Li Y B, Zheng M J, Ma L and Shen W Z 2006 *Nanotechnology* **17** 5101
[18] Li Y B, Zheng M J and Ma L 2007 *Appl. Phys. Lett.* **91** 073109
[19] Masuda H, Yada K and Osaka A 1998 *J. Appl. Phys.* **37** L1340
[20] Chu S Z, Wada K, Inoue S, Isogai M and Yasumori A 2005 *Adv. Mater.* **17** 2115
[21] Lee W, Ji R, Gösele U and Nielsch K 2006 *Nat. Mater.* **5** 741
[22] Choi J, Luo Y, Wehrspohn R B, Hillebrand Schilling R J and Gösele U 2003 *J. Appl. Phys.* **94** 4757
[23] Nielsch K, Choi J, Schwirn K, Wehrspohn R B and Gösele U 2002 *Nano Lett.* **2** 677
[24] Ono S, Ichinose H and Masuko N 1992 *Corros. Sci.* **33** 841
[25] Thompson G E and Wood G C 1981 *Nature* **290** 230
[26] Yao Z W, Zheng M J, Ma L and Shen W Z 2008 *Nanotechnology* **19** 465705
[27] Varghese O K 2002 *J. Mater. Res.* **17** 1162
[28] Khanna V K and Nahar R K 1986 *J. Phys. D: Appl. Phys.* **19** L141
[29] O'Sullivan J P and Wood G C 1970 *Proc. R. Soc.* A **317** 511